SF2A 2019
P. Di Matteo, O. Creevey, A. Crida, G. Kordopatis, J. Malzac, J.-B. Marquette, M. N'Diaye, O. Venot (eds)

THE CIRCUMSTELLAR ENVELOPES OF CEPHEIDS AND THEIR IMPACT ON THE PERIOD-LUMINOSITY RELATIONSHIP IN THE JWST AND ELT ERA.

V. Hocdé[1], N. Nardetto[1], E. Lagadec[1], G. Niccolini[1], A. Domiciano de Souza[1], A. Mérand[2], P. Kervella[3] and A. Gallenne[4]

Abstract. Cepheids are the keystone of the extragalactic distance ladder since their pulsation periods correlate directly with their luminosity, through the Period-Luminosity (PL) relation (Leavitt & Pickering 1912). The discovery of the accelerated expansion of the Universe (Riess et al. 1998; 2011 Nobel prize) is largely based on the Cepheid distance ladder. However, the calibration of the PL relation is still suffering from systematics errors of at least 2% and it is the largest contributor on the Hubble constant H0 (Riess et al. 2016). These systematics could be partly due to the CircumStellar Envelopes (CSEs) of Cepheids discovered in the last decade by interferometry. Using Spitzer Space Telescope observations, we reconstruct the spectral energy distribution of 5 Cepheids and we report the observation of an infrared (IR) excess continuum. We show for the first time that the IR excess can be modeled by a free-free emission due to a thin circumstellar shell of ionized gas in the chromospheric region.

Keywords: Techniques : Spectrometry, Photometry – Infrared : CSE, ISM – Stars : Cepheids –

1 Introduction

The extragalactic distance ladder is still largely based on Cepheids PL relations, whose uncertainties on both zero point and slope are today one of the largest contributors to the error on H_0 (Riess et al. 2019). One possible bias could be due to IR excesses from CSEs such as the ones discovered using near- and mid-infrared interferometry around nearby Cepheids (Kervella et al. 2006; Mérand et al. 2006). These studies determined a CSE radius of about 3 stellar radii and a flux contribution in the K band ranging from 2% to 10% of the continuum, for medium- and long-period Cepheids. However, we still do not know how these CSEs are formed, neither their nature, nor their characteristics (density and temperature profiles, chemical composition...). This work aims at understanding the nature of these CSEs by reconstructing and modeling the IR excess of Cepheids.

2 Building the infrared excess using the SPIPS algorithm

SpectroPhoto-Interferometric modeling of Pulsating Stars (SPIPS) is a model-based parallax-of-pulsation code which includes photometric, interferometric, effective temperature and radial velocity measurements in a robust model fit (Mérand et al. 2015). SPIPS uses a grid of ATLAS9 atmospheric models* (Castelli & Kurucz 2003) to compute synthetic photometry to match those from the dataset. While the visible domain up to $\sim 1\mu$m are well described by the pulsational model, an IR excess, increasing with wavelength, is observed (see Fig. 1-left). This IR excess has been modeled by an *ad-hoc* analytic law (see green line in Fig. 1-left):

$$\mathrm{IR_{ex}} = \Delta\mathrm{mag} = m_{\mathrm{obs}} - m_{\mathrm{kurucz}} = \begin{cases} 0, & \text{for } \lambda < 1.2\mu\mathrm{m} \\ \alpha(\lambda - 1.2)^{\beta}, & \text{for } \lambda > 1.2\mu\mathrm{m} \end{cases} \quad (2.1)$$

[1] Université Côte d'Azur, Observatoire de la Côte d'Azur, CNRS, Laboratoire Lagrange, France, email : vincent.hocde@oca.eu
[2] European Southern Observatory, Karl-Schwarzschild-Str. 2, 85748 Garcing, Germany
[3] LESIA (UMR 8109), Observatoire de Paris, PSL, CNRS, UPMC, Univ. Paris-Diderot, 5 place Jules Janssen, 92195 Meudon, France
[4] European Southern Observatory, Alonso de Córdova 3107, Casilla 19001, Santiago 19, Chile
*http://wwwuser.oats.inaf.it/castelli/grids.html

with two parameters, α and β. In the next section we reconstruct the IR excess up to 30μm owing to *Spitzer* space telescope observations. Our study aims to physically explain the behaviour of this IR excess, which is likely due to CSE.

3 Spitzer data

In order to study the IR excess of Cepheids we selected a sample of Galactic Cepheids with *Spitzer* observations (Werner et al. 2004). The spectroscopic observations were made with the InfraRed Spectrograph IRS (Houck et al. 2004) onboard the *Spitzer* telescope and the full spectra were retrieved from the CASSIS atlas (Lebouteiller et al. 2011).

We derive the IR excess of each star in the sample at the specific phase of *Spitzer* using:

$$\Delta\mathrm{mag} = m_{Spitzer} - m_{\mathrm{kurucz}}[\phi_{Spitzer}] \tag{3.1}$$

where $m_{Spitzer}$ is the magnitude of the *Spitzer* observation and $m_{\mathrm{kurucz}}[\phi_{Spitzer}]$ is the magnitude of the ATLAS9 atmospheric model interpolated at the phase of *Spitzer* observations ($\phi_{Spitzer}$). The $T_{\mathrm{eff}}(\phi)$ and $\log g(\phi)$ values of the star at the phase of *Spitzer* are provided by the SPIPS algorithm, while the interpolation is then done in a ATLAS9 grid of models with steps of 250K in effective temperature and 0.5 in log g, respectively. The angular diameter derived by SPIPS is then used to calculate $m_{\mathrm{kurucz}}[\phi_{Spitzer}]$. For V Cen we obtained the IR excess presented in Fig. 1-right. The observed discontinuity at 14μm is due to the different aperture sizes of *Spitzer* short and long wavelengths detectors. We also identify a silicate absorption around 10μm which could obscures a silicate emission from CSE. Therefore it is necessary to correct for the spectra from interstellar silicate absorption for studying the IR excess from CSEs.

4 Correcting for the interstellar silicate absorption in Spitzer data

In order to correct for the Spitzer spectra from interstellar silicate absorption we first derived the visible absorption A_{v} assuming an extinction law $A_{\mathrm{v}} = R_{\mathrm{v}}E(B-V)$ with a ratio of total-to-selective extinction of $R_{\mathrm{v}} = 3.1$, which corresponds to a diffuse ISM along the line of sight (Savage & Mathis 1979). Then we used the relation $A_{\mathrm{v}}/\tau_{9.7} = 18.5$ (Roche & Aitken 1984) which is suited to the diffuse ISM in the solar vicinity, in order to derive $\tau_{9.7}$. We obtain the following equation for the diffuse ISM:

$$A_{9.7}^{\mathrm{ISM}} = 1.086\tau_{9.7} = 1.086\frac{3.1}{18.5}\,E(B-V) = 0.182\,E(B-V), \tag{4.1}$$

Once we derived the specific absorption at 9.7μm, we can use this value to normalize a synthetic silicate absorption model in order to correct the entire *Spitzer* observations. Since we assumed an average ISM temperature of 20K, the dust emission is negligible in the *Spitzer* wavelength range according to Wien's law. Thus, we simply derive the absorption A_λ^{ISM} analytically using Mie theory. Hence we adopted the following expression for λ between 5 and 30μm:

$$A_\lambda^{\mathrm{ISM}} \propto \kappa_\lambda = \int C_\lambda^{\mathrm{abs}}(a)\pi a^2 n(a)\mathrm{d}a \tag{4.2}$$

We first derived C_λ^{abs} using complex refractive index for silicates from Draine & Lee (1984) (hereafter DL84) assuming an uniform distribution of ellipsoidal shapes given by Bohren & Huffman (1983). Then we derived the absorption coefficient κ_λ by taking into account a standard grain size distribution $n(a) \propto a^{-3.5}$ (Mathis et al. 1977). Finally we normalize A_λ^{ISM} using its specific value $A_{9.7}^{\mathrm{ISM}}$ at 9.7μm. Correction is presented in Fig. 1.

5 The IR excess from a thin shell of ionized gas

The shape of the mid-IR excess, saturating to a constant flux ratio at large wavelengths (see Fig. 2), suggests an opacity source increasing with wavelength. We used the free-free and bound-free opacities for a pure H shell presenting such behaviour. We consider the emission of a thin gas shell around the star with constant density and temperature for the sake of simplicity. The combined absorption coefficient (in m^{-1}; SI(MKS) unit system) for these two opacities sources is given by (e.g. Rybicki & Lightman 2008)

$$\kappa_\lambda = 3.692\times10^{-2}\left[1-\mathrm{e}^{-\frac{hc}{\lambda k T_{\mathrm{s}}}}\right] T_{\mathrm{s}}^{-1/2}\times(\lambda/c)^3(\gamma\rho/m_{\mathrm{H}})^2[g_{\mathrm{ff}}(\lambda,T_{\mathrm{s}})+g_{\mathrm{bf}}(\lambda,T_{\mathrm{s}})] \tag{5.1}$$

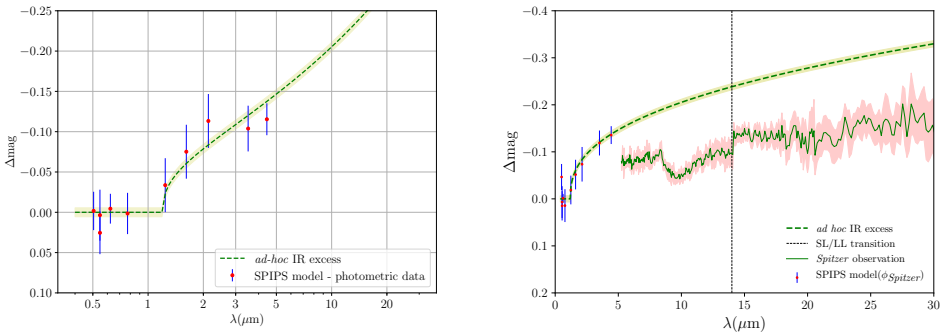

Fig. 1. Left: IR excess analytic law (Eq. 2.1) for V Cen together with the measurements. For each photometric band, red dots with error bars are the mean excess value over the cycle of the Cepheid and the corresponding standard deviation. The green zone is the error on the magnitude obtained using the covariance matrix of SPIPS fitting result. **Right:** *Spitzer* IR excess derived from Eq. 3.1. Red points are SPIPS interpolated IR excesses at the specific Cepheid phase of *Spitzer* observation. The transition between SL and LL detectors is indicated by a dashed line at $\sim 14\mu m$. The cycle-averaged *ad-hoc* analytic laws from SPIPS are represented by a dashed green for comparison only.

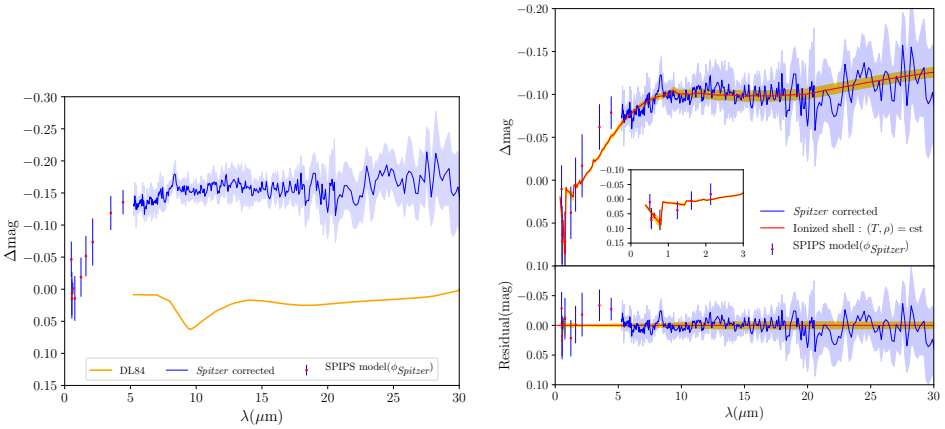

Fig. 2. Left: The IR excess of V Cen is presented, including (1) the interpolated IR excess model from SPIPS, (see Sect. 2), (2) the *Spitzer* observations cleaned from different camera effects and also corrected from the silicate absorption due to the ISM (orange curve see Sect. 4). **Right:** IR excess fitting results of a shell of ionized gas presented with residuals. Yellow region is the error on the magnitude obtained using the covariance matrix of the fitting result.

where h, c, and k have their usual meanings, γ is the degree of ionization (between 0 and 1), T_s the temperature of the shell, m_H the hydrogen mass and g_{ff} and g_{bf} are the free-free and bound-free Gaunt factors respectively. These factors were computed mainly from approximation formulas given by Brussaard & van de Hulst (1962), Hummer (1988), and references therein. We computed the SED of the star plus the gas shell taking into account the latter absorption coefficient κ_λ. In order to match the SPIPS photometries plus corrected *Spitzer* spectra we performed a χ^2 fitting using the Levenberg-Marquardt method. We fitted three parameters from the gas shell *i.e.* ionized shell mass γM_s, its temperature T_s and radius R_s. In addition, since the SPIPS fitting assumes that there is no excess in the visible it is necessary to relax this assumption to allow the data to present deficit or excess in the visible depending on the physical behaviour of the ionized shell. We fitted a fourth parameter corresponding to the IR excess offset corresponding to $\mathbf{\Delta m} \neq 0$ for $\lambda < 1.2\mu m$. Results are presented in Fig. 2 in the case of V Cen only. We show that we can reproduce the IR excess with a thin shell of ionized gas with a temperature ranging from 3500 to 4500K depending on the Cepheid considered, with a width of typically $\simeq 15\%$ of the radius of the star. In the case of V Cen, we obtain $T_{\rm shell} = 4353 \pm 106$K, $R_{\rm shell} = 1.156 \pm 0.012\ R_{\rm star}$, $\gamma M_{\rm shell} = 3.61.10^{-9} \pm 2.0.10^{-10} M_\odot$ and Δm=0.057 ± 0.004.

6 Conclusion and perspectives

For the five Cepheids we studied, we report a continuum IR excess increasing up to ∼-0.1/-0.2 magnitudes at 30μm, which cannot be explained by a hot or cold dust model of CSE. We show for the first time that IR excesses of Cepheids can be explained by free-free emission from a thin shell of ionized gas with a thickness of ≃8-17% star radius, an ionized mass of $10^{-9} - 10^{-7}$M$_\odot$ and a temperature of 3500-4500K. In this simple model, density and temperature have a constant radial distribution.

Interferometric observations have resolved CSEs around Cepheids. These CSEs were modeled with a ring at a distance of 2 to $3R_\star$, i.e. close to the star, in a region where the temperature is high enough ($> 2000K$) to prevent dust condensations. Thus, these observations are more likely explained by a shell of partially ionized gas. In parallel, it is interesting to compare Cepheids to very long period Mira stars for which a radiosphere near $2R_\star$ due to free-free emission has been reported (Reid & Menten 1997). Also, extensive studies of Hα profiles in the atmosphere of Cepheids have shown that strong increases of turbulence occurs when the atmosphere is compressed during its infalling movement, or because of shock waves dynamics (see for instance Breitfellner & Gillet (1993)). Moreover the analytical work of Neilson & Lester (2008) have shown that mass loss is enhanced by pulsations and shocks in the atmosphere. We suggest this mass loss could be in the form of partially ionized gas. The model of the shell of ionized gas could also be linked to the chromospheric activity of Cepheids. For example, Sasselov & Lester (1994) report HeIλ10830 observation on seven Cepheids providing the evidence of a high temperature plasma and steady material outflow in the highest part of the atmosphere.

However our model does not take into account temperature nor density gradients in the star's atmosphere, and in particular compression and/or shock waves which could also heat up the shell and ionize the gas. Thus, a spatial and chromatic analysis of the shell including interferometric constrains in all available bands with in particular VEGA/CHARA (visible), PIONIER/VLTI (infrared) and MATISSE/VLTI (L, M, N bands) is still necessary to better understand the environment of Cepheids, and eventually, check the impact on the PL relation.

The authors acknowledge the support of the French Agence Nationale de la Recherche (ANR), under grant ANR-15-CE31-0012-01 (project UnlockCepheids).

References

Bohren, C. F. & Huffman, D. R. 1983, Absorption and scattering of light by small particles (New York: Wiley, 1983)

Breitfellner, M. G. & Gillet, D. 1993, A&A, 277, 553

Brussaard, P. J. & van de Hulst, H. C. 1962, Reviews of Modern Physics, 34, 507

Castelli, F. & Kurucz, R. L. 2003, in IAU Symposium, Vol. 210, Modelling of Stellar Atmospheres, ed. N. Piskunov, W. W. Weiss, & D. F. Gray, A20

Draine, B. T. & Lee, H. M. 1984, ApJ, 285, 89

Houck, J. R., Roellig, T. L., van Cleve, J., et al. 2004, ApJS, 154, 18

Hummer, D. G. 1988, ApJ, 327, 477

Kervella, P., Mérand, A., Perrin, G., & Coudé du Foresto, V. 2006, A&A, 448, 623

Lebouteiller, V., Barry, D. J., Spoon, H. W. W., et al. 2011, ApJS, 196, 8

Mathis, J. S., Rumpl, W., & Nordsieck, K. H. 1977, ApJ, 217, 425

Mérand, A., Kervella, P., Breitfelder, J., et al. 2015, A&A, 584, A80

Mérand, A., Kervella, P., Coudé du Foresto, V., et al. 2006, A&A, 453, 155

Neilson, H. R. & Lester, J. B. 2008, ApJ, 684, 569

Reid, M. J. & Menten, K. M. 1997, ApJ, 476, 327

Riess, A. G., Casertano, S., Yuan, W., Macri, L. M., & Scolnic, D. 2019, arXiv e-prints

Roche, P. F. & Aitken, D. K. 1984, MNRAS, 208, 481

Rybicki, G. B. & Lightman, A. P. 2008, Radiative processes in astrophysics (John Wiley & Sons)

Sasselov, D. D. & Lester, J. B. 1994, ApJ, 423, 777

Savage, B. D. & Mathis, J. S. 1979, ARA&A, 17, 73

Werner, M. W., Roellig, T. L., Low, F. J., et al. 2004, ApJS, 154, 1